NAL TR-1244T

ISSN 0389-4010
UDC 533.6.011.3
533.6.04
533.6.69

TECHNICAL REPORT OF NATIONAL AEROSPACE LABORATORY

TR-1244T

Numerical and experimental study of drag characteristics of two-dimensional HLFC airfoils in high subsonic, high Reynolds number flow

Yoji ISHIDA, Masayoshi NOGUCHI,
Mamoru SATO and Hiroshi KANDA

JULY 1994

NATIONAL AEROSPACE LABORATORY

CHŌFU, TOKYO, JAPAN

This document is provided by JAXA.

Numerical and experimental study of drag characteristics of two-dimensional HLFC airfoils in high subsonic, high Reynolds number flow*

Yoji ISHIDA*1, Masayoshi NOGUCHI*1, Mamoru SATO*1 and Hiroshi KANDA*1

ABSTRACT

Hybrid laminar flow control (HLFC) is one of the most promising aircraft drag reduction technologies. However, very few experimental and theoretical studies have been reported. We have investigated both numerically and experimentally the aerodynamic characteristics of an HLFC airfoil and wing at high subsonic, high Reynolds number conditions. In this paper, we report the results of the wind tunnel test on drag characteristics, with and without suction, of two-dimensional HLFC airfoils with porous and slot suction approach under some adverse factors against laminar flow, and a numerical analysis of the wind tunnel data, which is based on the boundary layer calculation with a new transition prediction method allowed for the adverse factors and the Squire-Young drag formula. The HLFC models achieved total drag reduction of as high as 20% at realistic flight condition and the numerical method has given satisfactory predictions.

Keywords : Hybrid Laminar Flow Control, Airfoil, Subsonic flow, High Reynolds number flow,

ハイブリッド層流制御(HLFC)は実用上最も有望な航空機抵抗低減技術であるが、これまで理論、実験の両面から系統的に行われた研究は極めて少ない。我々は高亜音速、高レイノルズ数に於けるHLFC翼の空力特性を理論的、実験的に研究しているが、本報告では研究の出発点として、多孔、多溝各吸い込み表面を備えた二次元HLFC翼の、吸い込み有りと無しの場合の抵抗特性の風洞試験結果と、風洞試験において観察された自由流れや模型表面の粗さの影響を考慮に入れた新しい遷移点判定法と境界層計算とを組合わせてた数値計算法による実験データの数値解析の結果について報告する。我々のHLFC翼は、実機飛行条件に近いマッハ数およびレイノルズ数条件において、20%を超える全抵抗(ウエーク抵抗と等価吸い込み抵抗の和)の低減を実現出来た。また数値解析は全般的に満足すべき予測を与えた。

Nomenclature

A	damping length constant
c	chord length
C_1	a function of roughness height
C_2	a function of freestream turbulence intensity
C_{Di}	wake drag element
C_{DS}	equivalent suction drag coefficient
C_{DT}	total drag coefficient, $=C_{DW}+C_{DS}$
C_{DW}	profile drag coefficient
C_L	lift coefficient
C_P	pressure coefficient
C_Q	total suction quantity coefficient
H	total enthalpy or shape factor (only in eqs.8 and 9)
k	roughness height
M_∞	Mach number
P_{rt}	turbulent Prandtl number
Rc	chord Reynolds number
T	temperature
T'	freestream turbulence intensity
u	x component of mean velocity
u_k	u at y=k
u_τ	friction velocity
u', v'	fluctuation velocities
Ue	local freestream velocity
U_∞	freestream velocity
v_w	suction velocity
x,y	Cartesian coordinates
α	angle of attack
γ_{tr}	Chen-Thyson's intermittency factor
γ	boundary layer intermittency factor

* (received 11 April 1994)

*1 Aircraft Aerodynamics Division

This document is provided by JAXA.

δ boundary layer thickness
ε eddy viscosity
ε_t eddy conductivity
θ momentum thickness
$\varkappa$ total drag reduction rate
ρ density
μ viscosity coefficient
ν kinematic viscosity coefficient

Subscripts
te trailling edge
w wall condition
Superscripts
$(\bar{})$ time averaged quantity, or transformed incompressible plane

1. INTRODUCTION

Aircraft drag reduction by means of hybrid laminar flow control (HLFC) which combines natural laminar flow (NLF) and laminar flow control (LFC) has got much attention in aeronautical sciences owing to the possibility of achieving extensive laminar region on a wing with simpler system[1]. Recently, practicality of the HLFC concept for realistic flight applications was tried successfully on a 757 aircraft[2]. However it showed that further flight and wind tunnel tests are necessary to develop the system with high reliability even at off-design condition. As far as the present author knows, very few wind tunnel tests have reported the performance of HLFC airfolis in the realistic flight conditions. This is the motive of the experimental study.

As the first stage of the experimental study, we have executed the high subsonic, high Reynolds number wind tunnel test of two-dimensional HLFC airfoils to get their drag characteristics at the design and off-design conditions. Unfortunately, as some authors pointed out, severe adverse factors against laminar flow were recognized in the test : freestream turbulence, contamination of the surface due to impacts of particles in the flow and surface roughness of suction hole or slot which is inevitable in the HLFC test. We found it difficult to estimate the effect of the adverse factors on drag without the aid of any accurate theoretical tool. It is the motive of the numerical study. We developed a numerical method which consists of the boundary layer solution with a new transition prediction method allowed for the adverse factors desribed above, and of a compresible version of Squire-Young's drag formula. We then evaluated drag values of the HLFC airfoils and discussed problems in the wind tunnel test.

Finally, someone says that in relation to practical application of LFC, any two-dimensional test may be meaningless. Our answer to the quetion is that apart from its intrinsic interest, the two-dimensional HLFC study is necessary to investigate the problem of controlling the three-dimensional boundary layer over a wing whose cross flow instability in the leading edge region is already suppressed by suction.

2. OUTLINE OF THE WIND TUNNEL TEST

We will describe here the outline of the wind tunnel test. The reader is referred to ref.15 for further details of it.

2.1 AIRFOIL MODELS

Figure 1 shows geometric outline of the model. Basic airfoil section is 'NLAM78', a natural laminar flow airfoil[3], whose design Mach number M_∞ and lift coefficient C_L is 0.77 and 0.50, respectively. The chord length is 0.25m and the span 0.30m. The suction region was decided to range from 40 to 80% chord of the upper surface of the models with reference to the result of the flight test[3] at Reynolds number $Rc=20\times10^6$. Two suction approach, porous and slot, were tested to compare their drag reduction performance. The porous suction panel has many fine holes of diameter of 0.1mm and spacing of 0.7mm and the slot fine spanwise slots of width of 0.1mm and chordwise spacing of 5mm. Both panels have same open area ratio.

Structural restrictions prevented us from realizing full span suction surface, thereby two-dimensional flow over the model was lost except the central region of it. Hence the wake survey to evaluate the profile drag was made in the symmetrical plane of the model. Besdes the suction surface models we also used a solid surface model with same airfoil section and a surface pressure tap row to measure surface pressure distribution and basic drag value to be compared with those of the suction models[20].

2.2 TEST CONDITIONS

This document is provided by JAXA.

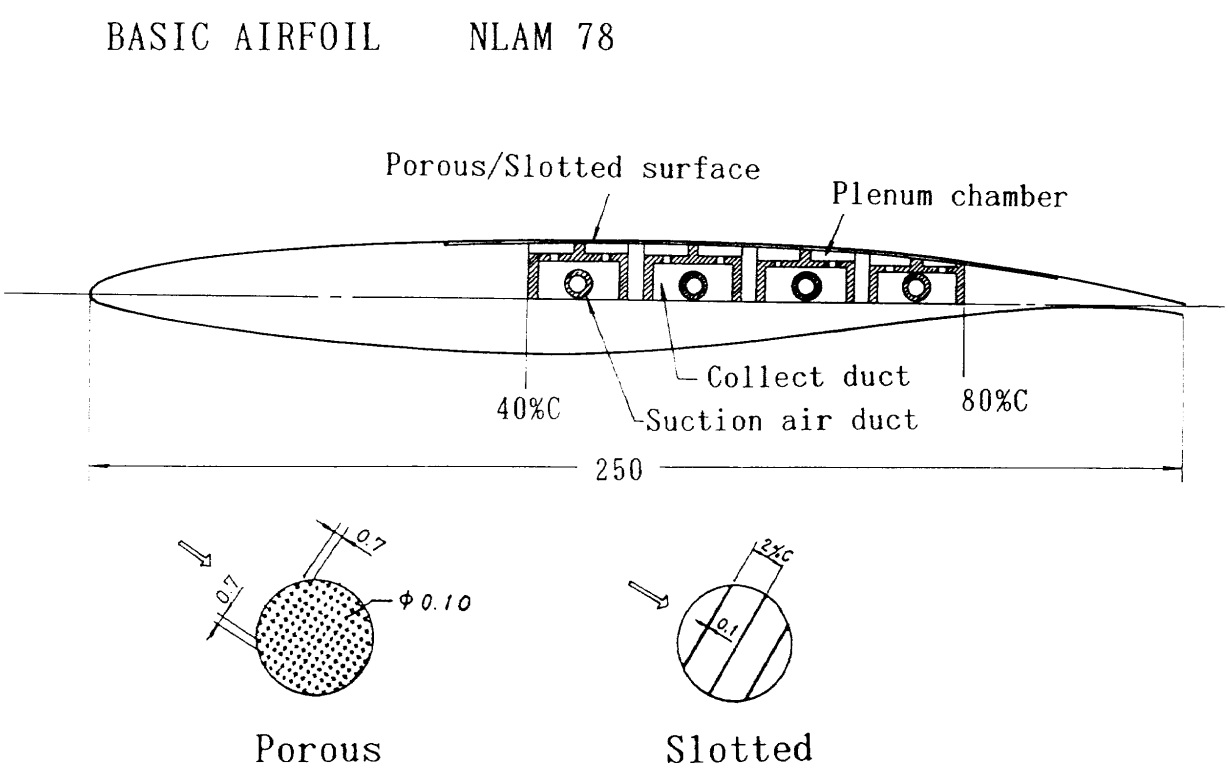

Figure 1.(a) Airfoil section with suction chamber and ducts

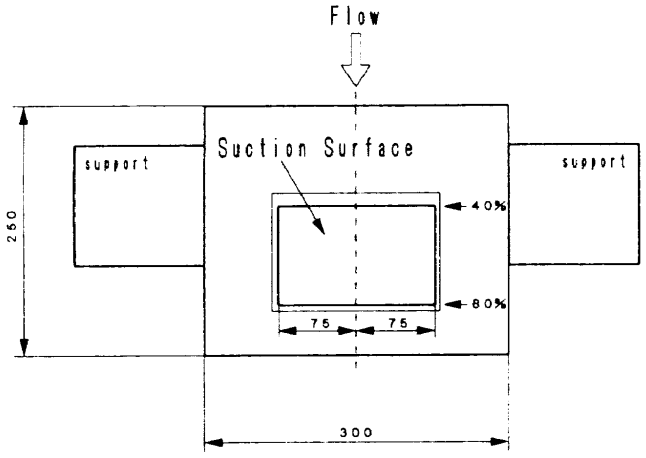

Figure 1.(b) Dimension of the test models

We have conducted the test at the NAL two-dimensional transonic wind tunnel, whose maximum Mach and Reynolds numbers are 1.1 and 40×10^6, respectively and the test section has a width of 0.3m and a height of 1.0m. The freestream turbulence intensity including both vortical and acoustic modes was estimated to be about 1%[4] (see also figure 3). We measured the surface pressure distribution as well as the profile drag with and without suction, for M_∞ from 0.60 to 0.82, Rc from 6 to 20 million and angle of attack from -2° to $+2^\circ$; all the measurements were executed in transition free condition. We applied unifrom chordwise suction quantity with various levels for the suction tests, and hence tried no suction quantity optimization. We corrected all of the measured drag data for the wind tunnel wall interference effect by Sawada's method[5].

2.3 TEST RESULTS

We will present the results of the wind tunnel test in the section "RESULTS", together with the results of the numerical analysis with the method which is described in next section.

3. NUMERICAL METHOD

The profile drag was computed by Squire-Young's formula for compressible flows[13], which required boundary layer parameters at the trailing edge. To get them, we solved the two-dimensional compressible boundary layer and energy equations with Keller Box schem[6] for laminar and turbulent flow regions, predicting the transition location based on the new empirical method which accounts for the adverse factors above described, from the forward stagnation point to the trailing edge.

3.1 PREDICTION OF THE TRANSITION POINT

In the analysis of the present wind tunnel data it is

This document is provided by JAXA.

crucial to account for the effects of freestream turbulence and wall roughness on the transition location. However very few empirical criterions allow for both of them, although some ones integrate only the effect of freestream turbulence (Arnal et.al[7], van Driest & Blummer[8]). Modification of the e^N method to include the effects still remains unsatisfactory. The approach which uses turbulence model equations to follow downstream a specified disturbance introduced into the laminar boundary layer has been carried out by several authors (MacDonald and Fish[9], Forest[11], Finson[12] and Simon & Stephens[10]). MacDnald-Fish and Finson used differential models which intergrate both roughness and freestream tubulence to well predict the transition point. Their models, however, are rather too complicated to examine their validity for the weak disturbance in the laminar layer.

We used the turbulence model equation approach with two alterations : the first is that a compressible version of Michel's criterion (see Appendix) is used to predict the transition point and the second is that we elaborate a new simpler eddy viscosity model which is expressed as

$$\frac{\varepsilon}{\nu}=\begin{cases}\dfrac{0.16y^2}{\nu}\left[1-\exp\left(-\dfrac{y}{A}\right)\right]^2\dfrac{\partial u}{\partial y}, & \text{(1a)}\\ C_1\left(\dfrac{u_\tau k}{\nu_w}\right)^2\dfrac{\nu_w}{\nu}+C_2T'\dfrac{U_\infty\delta}{\nu}. & \text{(1b)}\end{cases}$$

The innner layer model, eq.(1a), is exactly the standard mixing length one, which satisfy the wall boundary condition for $-\overline{\rho u'v'}$. The outer layer model, eq.(1 b), consists of two terms : the first represents the influence of roughness and the second freestream turbulence. We assumed that each term is proportional to the product of typical velocity and length of each phenomena : $u_k \cdot k$ for the roughness and $u'\delta$ for the freestream turbulence. Then if the roughness heigh is small, u_k can be exprseed approximately as

$$u_k \sim (\partial u/\partial y)_0 \cdot k = u_\tau^2 k/\nu_w,$$

and thus

$$\frac{u_k k}{\nu}=\frac{u_\tau k}{\nu_w}\cdot\frac{u_\tau k}{\nu}=\left(\frac{u_\tau k}{\nu_w}\right)^2\frac{\nu_w}{\nu}.$$

By using the definition of T', i.e. $u'=T'\cdot U_\infty$,

$$u'\delta/\nu = T'U_\infty\delta/\nu$$

Then eq.(1b) results. The factors C_1 and C_2 in eq.(1b) were decided empirically as a function of k and T', respectively, by using the data of Feint[16] and flat plate with freestream turbulence[17] as shown in figure

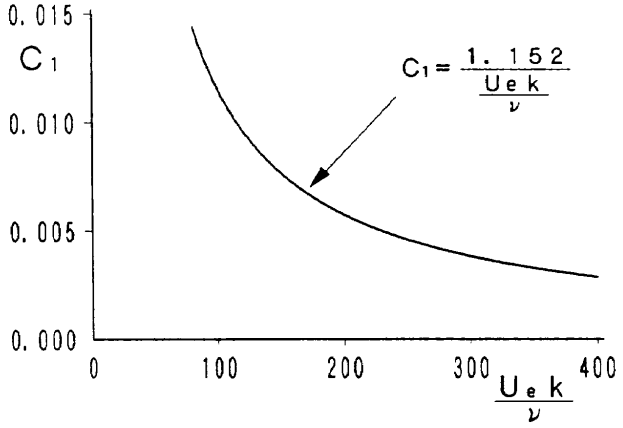

Figure 2.(a)

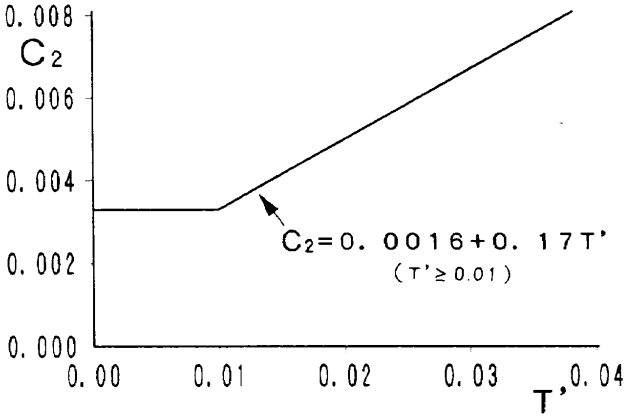

Figure 2.(b) Cofficients C_1 and C_2 appeared in eqation 1(b)

2. Note that the eddy viscosity model is applied only in the laminar layer region.

3.2 TURBULENCE MODEL

Eddy viscosity and eddy conductivity concepts are used in the method which are defined as

$$-\overline{\rho u'v'}=\rho\varepsilon\,(\partial u/\partial y) \qquad \text{(2a)}$$

$$-\overline{\rho v'H'}=\rho\varepsilon_t(\partial H/\partial y)=\rho\,(\varepsilon/P_{rt})\,(\partial H/\partial y), \qquad \text{(2b)}$$

where u is the mean velocity, H the total enthalpy, ρ the density and P_{rt} turbulent Prantdl number. We used Cebeci-Smith's eddy viscosity model including effects of both suction and roughness, and compressibility[6] :

$$\varepsilon=\begin{cases}0.16(y+\Delta y)^2\{1-\exp[-(y+\Delta y)/A]\}^2\times & \\ \quad|\partial u/\partial y| & 0\leqq y\leqq y_i\\ & \text{(3)}\\ 0.0168\left|\int_0^\infty(Ue-u)dy\right|\cdot\gamma(y/\delta) & y_i<y<\delta\end{cases}$$

where y_i is a y ordinate of a point of intersection of the two curves and

This document is provided by JAXA.

$$
\left.\begin{aligned}
&A=26\frac{\bar{\nu}}{N}\left(\frac{\tau_w}{\rho_w}\right)^{-\frac{1}{2}}\left(\frac{\bar{\rho}}{\rho_w}\right)^{\frac{1}{2}}\\
&N^2=\frac{\bar{\mu}}{\mu_e}\left(\frac{\rho_e}{\rho_w}\right)^2\frac{p^+}{v_w^+}\left[1-\exp\left(11.8\frac{\mu_w}{\bar{\mu}}v_w\right)\right]\\
&\quad+\exp\left(11.8\frac{\mu_w}{\bar{\mu}}v_w\right)\\
&p^+=\frac{\nu_e U_e}{u_\tau^3}\frac{dU_e}{dx},\quad v_w^+=\frac{v_w}{u_\tau},\quad u_\tau=\left(\frac{\tau_w}{\rho_w}\right)^{\frac{1}{2}}\\
&\Delta y=\begin{cases}0.9\dfrac{\nu}{u_\tau}\left[\sqrt{k_s^+}-k_s^+\exp(-k_s^+/6)\right] & (k_s^+\leqq 70)\\ 0.7\dfrac{\nu}{u_\tau}(k_s^+)^{0.58} & (k_s^+>70)\end{cases}\\
&k_s^+=u_\tau k/\nu\\
&\gamma=\left[1+5.5(y/\delta)^6\right]^{-1}
\end{aligned}\right\}\quad(4)
$$

For transitional region, we multiply ε by Chen and Thyson's intermittecy factor γ_{tr} :

$$\gamma_{tr}=1-\exp\left[G\cdot(x-x_{tr})\int_{x_{tr}}^{x}\frac{dx}{U_e}\right]\qquad(5)$$

where

$$
\left.\begin{aligned}
&G=\frac{3}{C^2}\frac{U_e^3}{\nu_w^2}\left(\frac{U_e x_{tr}}{\nu_w}\right)^{-1.34}\\
&C=60+4.86\ Me^{1.92}\quad(0\leqq Me\leqq 5)
\end{aligned}\right\}\qquad(6)
$$

3.3 SQUIRE-YOUNG'S PROFILE DRAG FORMULA

The Squire-Young formula for compressible flow[13] is given by

$$C_{DW}=2\left[(\theta_\infty)_{upper}+(\theta_\infty)_{lower}\right]/c\qquad(7)$$

where

$$\theta_\infty=\theta_{t.e.}\left(\frac{\rho_e}{\rho_\infty}\right)_{t.e.}\left(\frac{U_e}{U_\infty}\right)_{t.e.}^{\frac{H_{t.e.}+H_\infty+4}{2}}\qquad(8)$$

$$H_\infty=1+(\gamma-1)M_\infty^2\qquad(9)$$

The formura is applicable to the case with suction, too.

4. ASSUMPTIONS IN THE CALCULATION

In all of the following calculations, it is assumed that the freestream turbulence intensity T' takes the value shown in figure 3, which was estimated from the measurment[4] ; the suction surfaces have distributed roughness with a height of half of the hole/slot dimension, k=0.05mm, which was decided from a comparison of drag between a rivet and a hole (Young and Paterson[21]) ; and the wall is adiabatic.

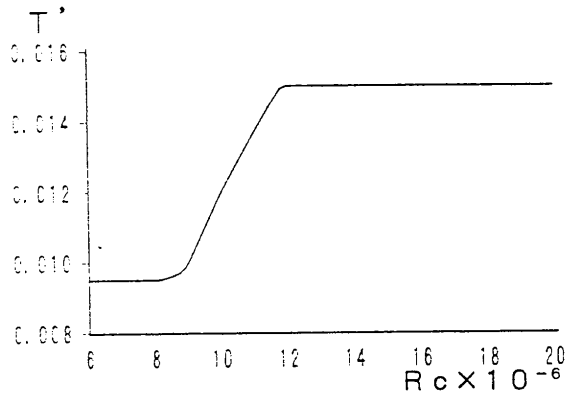

Figure 3. Freestream turbulence intensity assumed in the numerical analysis

5. RESULTS

5.1 SURFACE PRESSURE DISTRIBUTION

Figure 4(a) shows typical measured surface pressure coefficient Cp at the design Mach number (=

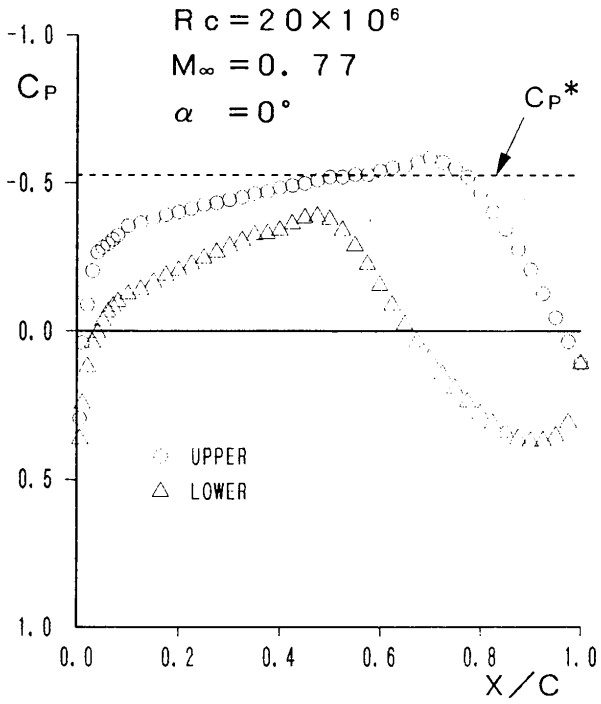

Figure 4.(a) Surface pressure coefficient Cp at design Mach number

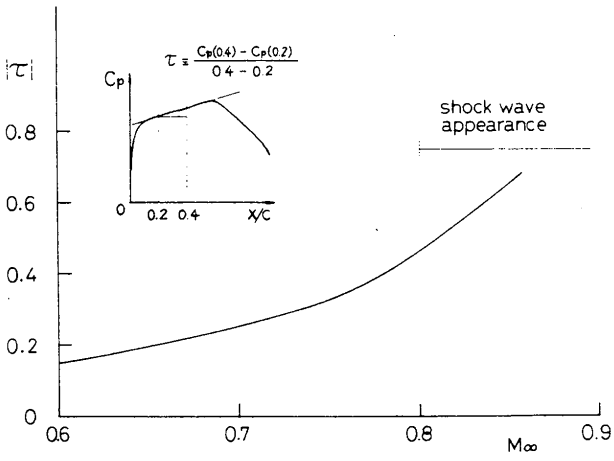

Figure 4.(b) Magnitude of favorable pressure gradient τ at $\alpha=0$

This document is provided by JAXA.

0.77) and angle of attack of zero. We can see that favorable pressure gradients extend up to 70% (upper surface) and 50% (lower surface) chord. All the data including the ones not presented show that the Cp at fixed M_∞ depends little on Reynolds number and the favorable pressure gradient at zero angle of attack depends much on Mach number ; it increases with Mach number as is shown in figure 4(b).

5.2 DRAG CHARACTERISTICS WITHOUT SUCTION

We first desribe the drag characteristics of the HLFC airfoils without suction, because they are the basic data to be compared with those with suction.

The measured profile drag coefficient C_{DW} is plotted against Mach number for Rc of 8 and 20 million in figure 5 together with the calculated results. The latter (solid and broken lines) gives consistently lower values than experiments, although qualitative agreement is excellent. The quantitative disagreement mainly comes from the tendency of the boundary layer method of underestimating (in average about 10 %) the momentum thickness at the trailing edge, on which the drag directly depends. Hence if the underestimation is allowed for, the agreement with experimental data would be much improved.

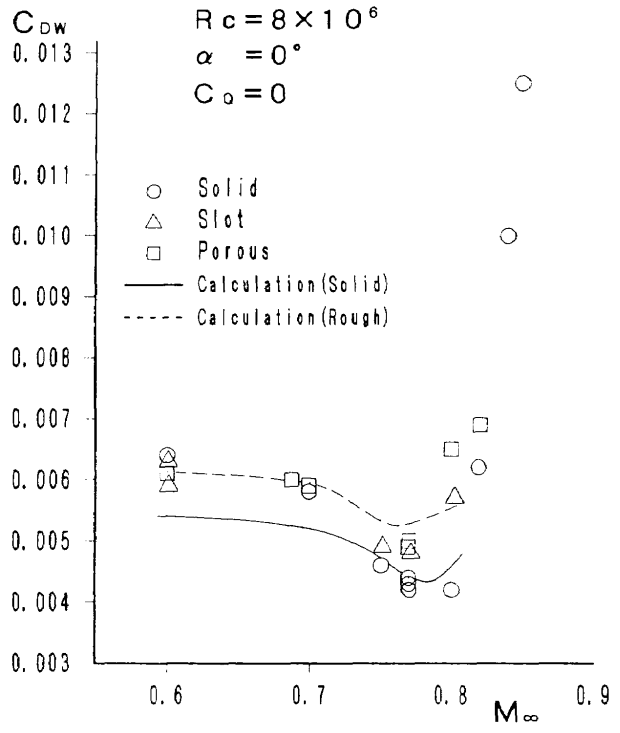

Figure 5.(a) Variation of the wake drags with Mach number when suction is not applied

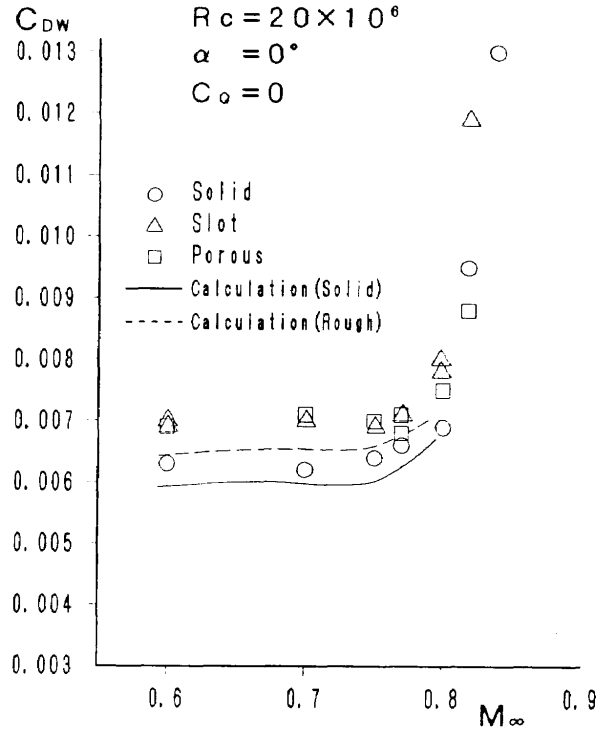

Figure 5.(b) Variation of the wake drags with Mach number when suction is not applied

Detailed observation of the experimental data reveals some unusual features of C_{DW}. The first one is that the drag values of the suction surface models (□, △) are consistently higher than that of the solid surface model(○). The second is that the variation of C_{DW} with Mach number at $Rc=8\times10^6$ is more complicated when compared with the one at 20×10^6 : it decreases rapidly with Mach number until it reaches minimum at the design Mach number of 0.77 and then rapidly increases again. What is the reason of the features? As the numerical method can predict correctly the features, the analysis of the numrical result would help us to answer the question : the first one is primarily due to the roughness effect of the suction surface, because the test conditions except airfoil surface are same for the three models when suction is not applied and the numerical analysis tells us the possibility that fairly thin boundary layer over the small, suction surface models in high Reynolds number flow makes even fine suction hole/slot a supercritical roughness. Then a question arises if it is an intrinsic problem of the suction LFC or only special one happen to appear in the wind tunnel test. It will be discussed later in 'DISCUSSION'.

This document is provided by JAXA.

The second feature contains more complex phenomena and the numerical analysis suggests that it is due to the combined effect of Reynolds number and the favorable surface pressure gradient on the transition location; at $Rc=8\times10^6$, the transition delaying effect of the favorable pressure gradient works well at the desigh Mach number at which low drag values are certainly attained, but becomes weaker rapidly as Mach number decreases from the desigh Mach number because of the decrease of the favorable pressure gradient (see figure 4b) which causes forward movement of the transition point, namely drag increase. At $Rc=20\times10^6$, on the other hand, the transition point is almost fixed near the leading edge region even at design Mach number, and thus the variation of C_{DW} with Mach number up to drag divergent Mach number becomes smaller.

Figure 6 shows the variation of C_{DW} with Reynolds number at the design Mach number ($M_\infty=0.77$). It is interesting to note that the C_{DW} increases rapidly at Reynolds number of about 10×10^6 and the roughness effect of the porous surface is also observed (see the difference between the solid and the porous models).

The calculated drag in figure 6 generally agrees well with the experiments for entire Reynolds number range, which is primarily due to the correct assumption of the freestream turbulence intensity T' (figure 3).

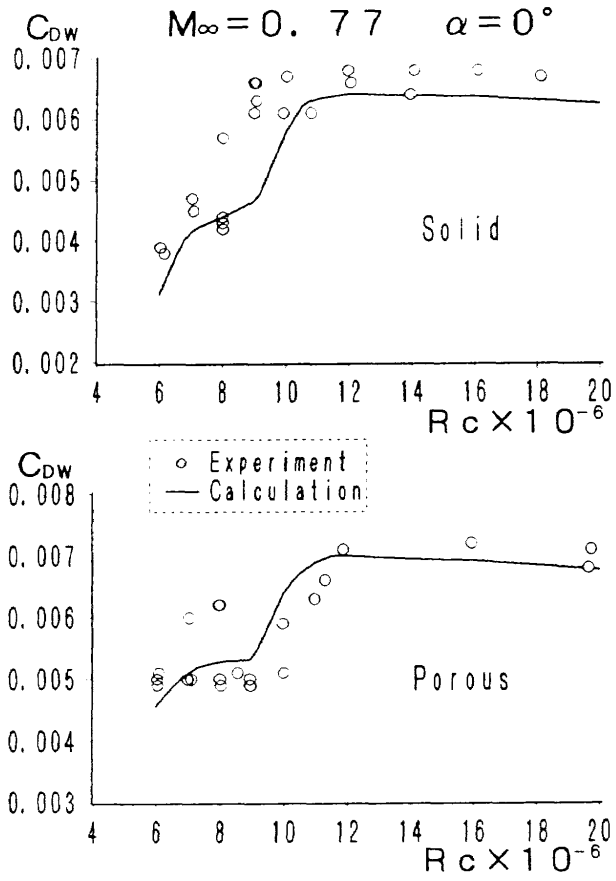

Figure 6. Variation of the wake drag with Reynolds number at the desigh Mach number when suction is not applied

5.3 DRAG CHARACTERISTICS WITH SUCTION

We first refer to the result at the desigh Mach number. In figure 7 the profile drag of the HLFC models with the suction applied in the midchord region (40~80% chord) is plotted against the total suction quatity coefficient C_Q, defined by

$$C_Q=\int_0^1(\rho_w v_w/\rho_\infty U_\infty)\ d(x/c). \tag{10}$$

The measured drag (○, △) decrease monotonously with C_Q up to 0.0006, the maximum one used in the test, even at $Rc=20\times10^6$. We also found no significant difference in the drag reducing effect between the porous and the slot suction approach.

The calculation gives a little lower values than the experiments, from the same reason stated previously,

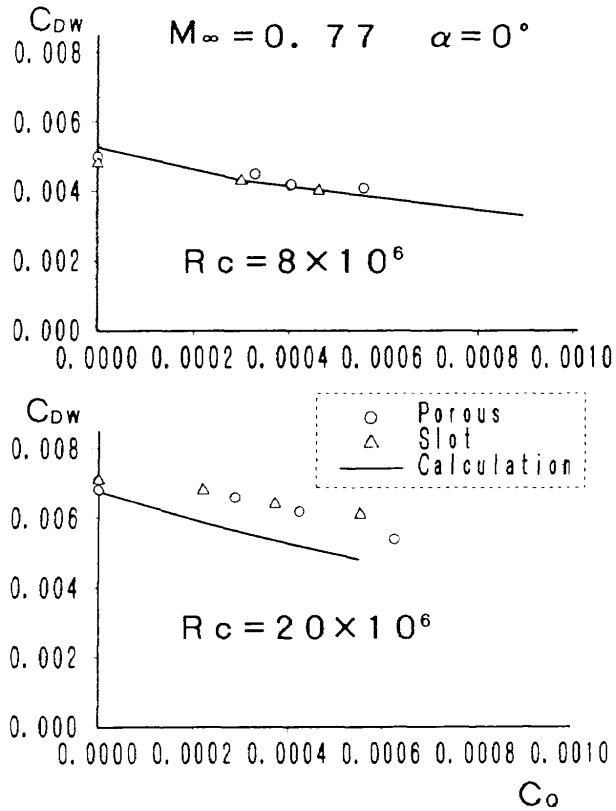

Figure 7. Effect of suction on the wake drag reduction at design Mach number. ○, △ : experiments.

This document is provided by JAXA.

and in addition a little larger value of $|dC_{DW}/dC_Q|$, i.e. larger drag reducing effect than the experiment, the reason of which is not yet fixed because of some uncertain factors in both the theoretical model and the experimental results.

In discussing net energy saving effect of suction LFC, we must consider the total drag coefficient C_{DT}, which is defined as the sum of the profile drag C_{DW} and the equivalent suction drag C_{DS}, which is calculated from eq.(13) of Ref.14. Then the total drag reduction rate $\kappa(\%)$ defined by

$$\kappa=100\times [C_{DT}(C_Q=0)-C_{DT}]/C_{DT}(C_Q=0) \qquad (11)$$

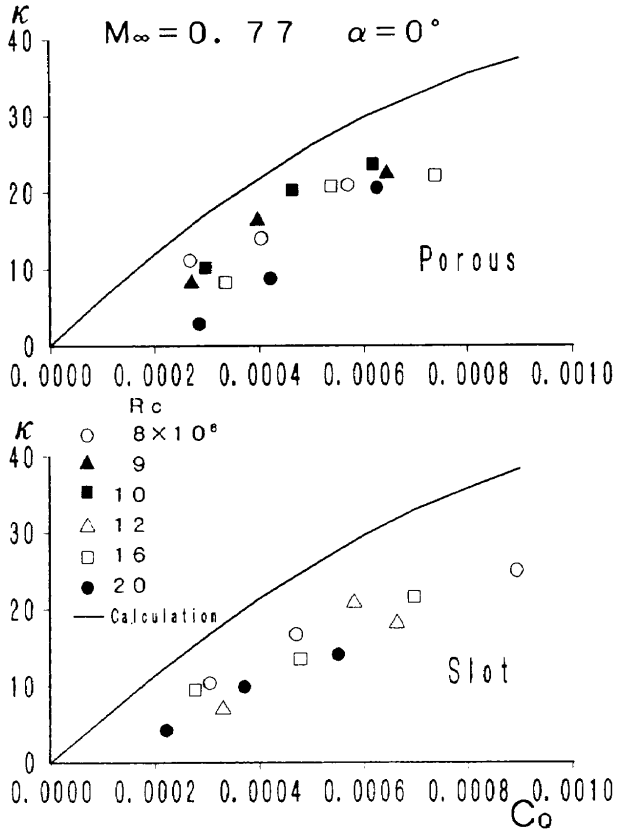

Figure 8. Total drag reduction rate at design Mach number

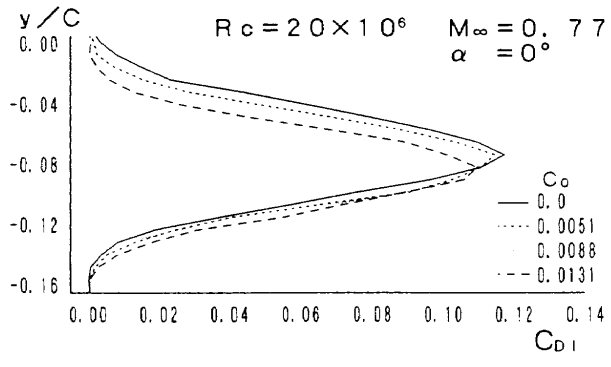

Figure 9. Wake drag element C_{Di}

is plotted against C_Q for various Reynolds numbers in figure 8. We can see from it that both models have the total drag reduction rate as high as 20%, still very high value. The calculation gives higher value (solid line).

Figure 9 shows profiles of wake drag element C_{Di} across the wake defined by

$$C_{DW}=\int_{-\infty}^{+\infty} C_{Di}\, d(y/c) \qquad (12)$$

The profile, which has rarely been used, can directly represent the effect of suction on the drag; the suction applied on the upper surface of the airfoil causes not only the reduction of the element C_{Di} mainly in the upper side the wake, but also some downward shift of the profile or equivalently wake flow with C_Q, which we suggest is intimately related to lift change (probably increase) caused by the boundary layer suction.

The profile drag C_{DW} measured at off-design Mach numbers of 0.6 and 0.8 also show monotonous reduction with C_Q, as is shown in figure 10. The total drag reduction rate κ of the porous models at Rc=8

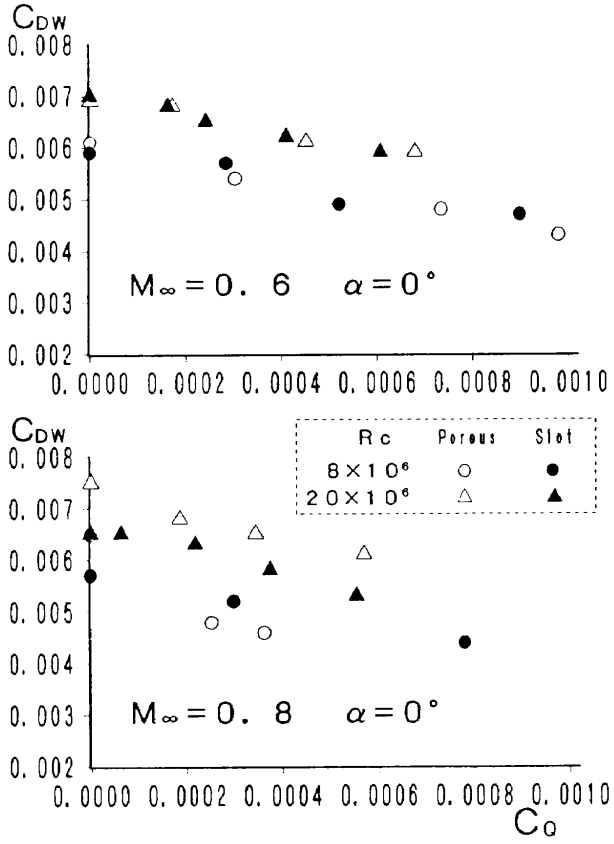

Figure 10. Effect of suction on the wake drag at off-design Mach numbers

This document is provided by JAXA.

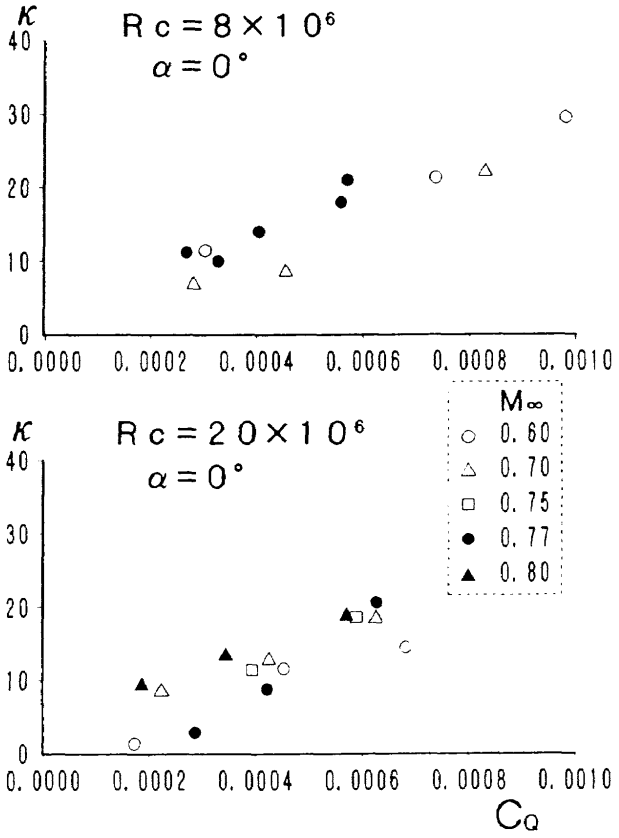

Figure 11. Total drag reduction rate at off-design Mach numbers

and 20 million are plotted in figure 11 for various Mach number, from which we can see that large amount of reduction was attained even at off-design conditions.

The achievement of such high total drag reduction rate in high subsonic, high Reynolds number flow is quite encouraging.

6. DISCUSSION

We will discuss here some problems which remain unsolved in the wind tunnel tests, with the aid of the numerical calculation.

The roughness effect of suction hole/slit found in figure 5 or 6 is very serious and perplexing problem in LFC and raised a question if the effect is intrinsic or not. As was stated above, the numerical analysis of the test showed that the roughness of suction hole/slit did not always remain subcritical owing to the very thin boundary layer developed on the surface of the small model in high Reynolds number flows. Thus it is expected that if a larger size model with the suction surface unchanged is used, the roughness effect would

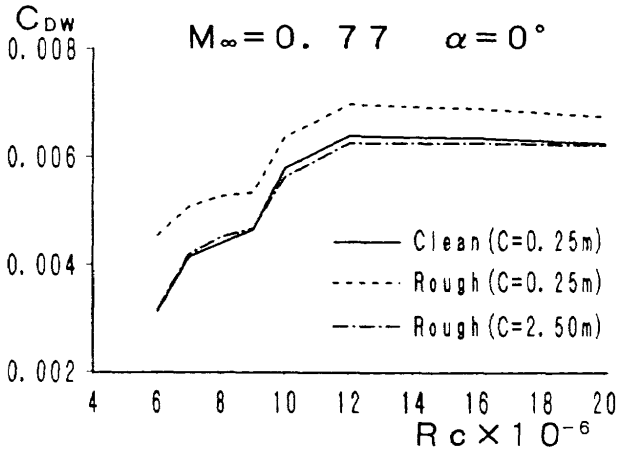

Figure 12. Calculated wake drag of the larger airfoil model compared with those of the present, small models with and without surface roughness

not appear. To support it, we computed the drag of the model with the chord length of 2.5m, ten times larger than the present one when suction is not applied, and compared the result with those of the present models in figure 12. It shows that the larger model has almost same drag as that of the small model with smooth surface ; the roughness effect is negligible for the larger model. Now we reach a conclusion that the roughness effect is only a particular one happen to be caused by the use of small model in high Reynolds number flow and is not intrinsic defect of HLFC/LFC airfoil. The ratio of the dimension of the suction hole/slit to the boundary layer thickness is an important parameter of HLFC/LFC test and must be kept constant if we want to compare data of different tests or extrapolate wind tunnel data to flight conditions, although it is not technically easy.

We have measured transition points over the upper surface of the slot surface model by flow visualization using temperaturesensing liquid cristals in the wind tunnel test.

Figure 13 represents the measured (△) and the calculated (lines) transition points at the design Mach number. The broken line exactly corresponds to the experimental case and the agreement is excellent, which proves the accuracy of the prediction method of the transition. In the figure the calculated transition point of the solid surface model is also ploteed (full line) : rapid forward movement of the point at Reynolds number near 10 million corresponds to

This document is provided by JAXA.

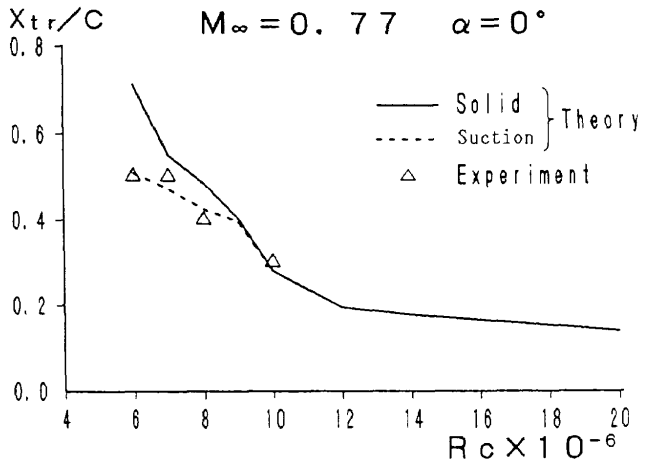

Figure 13. Comparison of the transition location between theory and experiment

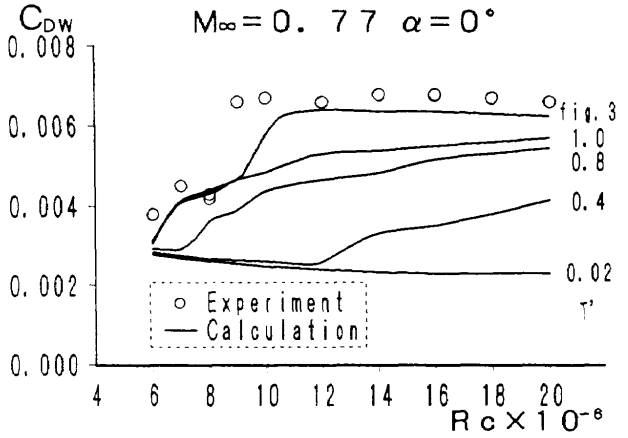

Figure 14. Effect of freestream turbulence intensity on the wake drag value (T' in percent value)

rapid increase of the drag there (figure 6). Departure of the computed transition curve of the suction surface model from that of the smooth model which begins at Rc of 9×10^6 reflects correctly the effect of the presence of suction surface roughness.

Figure 13 also shows that the transition of the suction surface model occurs ahead of the suction region ($x/c<0.4$) for Reynolds numbers greater than 9 million, which means that the suction is actually applied to the turbulent, not laminar, boundary layer. However the suction really reduced the drag significantly as is shown by the data at Rc of 20 million in figure 7. Thus the turbulent boundary layer suction succeeded in producing a large amount of drag reduction in the test. As far as the present author knows, very few papers have referred to the success of the drag reduction by means of turbulent boundary layer control with suction, so it is very important and encouraging result, especially considering the case of an accidental, temporal failure of laminarization caused by leading edge contamination by insect debris or ice and so on.

The effect of freestream tubulence intensity on the drag is well simulated by the numerical method. The result in figure 14 shows that the effect is significant and complicated ; thus the drag in realistic flight conditions with very low turbulence is hardly estimated from convensional wind tunnel test data without the aid of any accurate theoretical model.

7. SUMMARY

We have made a numerical and experimental study of the drag characteristics of the two-dimensional HLFC airfoils which combines 'NLAM78', a NLF airfoil, with the porous or slot suction approach in high subsonic, high Reynolds number flows. The main results of the wind tunnel test are as follows.

The HLFC airfoils achived the total drag reduction more than 20% with moderate suction quantity for Mach and Reynolds numbers up to 0.80 and 20×10^6, respectively, in spite of several adverse factors against laminar flow. No significant difference in drag characteristics with suction was found between the porous and the slot suction approach.

When suction is not applied, the suction surface models were found to give a little higher drag value than solid surface one due to the roughness effect of the suction surfaces. Combined effects of the favorable surface pressure gradient and the adverse effects against laminar flow caused complicated vaviation of the transition location, or the drag, with Mach number, especially at low Reynolds numbers.

Along with the wind tunnel test, we made the numerical analysis of the profile drag of the HLFC airfoils, which is based on the boundary layer solution with the new prediction method of the transition location taking into account of the adverse factors and Squire-Young's drag fromula for compressible flow. The analysis has generally given satisfactory qualitative agreement with the experimental data,

This document is provided by JAXA.

although it has consistently predicted a little lower drag values than the wind tunnel data with and without suction owing to the understimation of the momentum thickness at the trailing edge on which the drag value directly depends.

The calculation predicted the possibility of the turbulent boundary layer control by suction for Reynolds number greater than 9×10^6. The effects of the freestream turbulence and the surface roughness, whose detailed study in the wind tunnel test was difficult, were favorably discussed by the numerical method.

REFERENCES

1. R.W. Barnwell and M.Y. Hussaini ed., "Natural Laminar Flow and Laminar Flow Control," Springer-Verlag, 1991.
2. C.A. Shifrin, "Hybrid Laminar Flow Tests Cut Drag, Fuel Burn on 757", Aviation Week & Space Technology, Dec.2 1991, p.36
3. Boeing Commercial Airplane Company, "F-111 Natural Laminar Flow Glove Flight Test-Data Analysis And Boundary Layer Stability Analysis", NASA CR-166051 (1984).
4. Y. Oguni, M. Sato, H. Kanda, S. Sakakibara, H. Miwa and S. Baba, "Flow Quality of NAL Two-Dimensional Transonic Wind Tunnel, Part IV. Flow Turbulence Level and Measuring Method", (In Japanese) National Aerospace Laboratory TR-842 (1984).
5. H. Sawada, S. Sakakibara, M. Sato and H. Kanda, "Wall Interference Estimation of the NAL's Two-Dimensional Wind Tunnel", (In Japanese) National Aerospace Laboratory TR-829 (1984).
6. T. Cebeci and P. Bradshaw, "Physical and Computational Aspects of Convective Heat Tranfer". Springer-Verlag (1984).
7. D. Arnal, "Description and prediction of transition in two-dimensional incompressible flow". AGARD R-709, 'Special course on stability and transition of laminar flow,' (1984)
8. E.R. Van Driest and C.B. Blumer, "Boundary Layer Transition, freestream turbulence and pressure gradient effects". AIAA Jour. vol.1, No.6, p.1303, 1963
9. H. McDonald and R.W. Fish, "Practical Calculations of Ttansitional Boundary Layers". Int. J. Heat and Mass Transfer, vol.16, pp.1729-1744, 1973.
10. F.F. Simon and C.A. Stephens, "Modeling of the Heat Transfer in Bypass Transitional Boundary-Layer Flows", NASA Tech. Paper 3170, (1991).
11. A.E. Forest, "Engineering Predictions of Transitional Boundary Layers", AGARD CP-224, Laminar-Turbulent Transition (1977).
12. M.L. Finson, "On the application of second order closure models to boundary layer transition", AGRD CP-224, Laminar-Turbulent Transtion (1977).
13. A.D. Young, "Note on momentum methods of measuring profile drags at high speeds". ARC R & M 1963 (1940).
14. C.W. Brooks, Jr., C.D. Harris, and W.D. Harvey, "The NASA Langley Laminar-Flow-Control Experiment on a Swept, Supercritical Airfoil, Drag Equations". NASA TM 4096 (1989)
15. M. Noguchi, M. Sato, H. Kanda and Y. Ishida, "High subsonic and high Reynolds number wind tunnel tests of two-dimensional natural laminar flow airfoils with suction boundary layer control (In Japanese)". National Aerospace Laboratory TR-1204.
16. E.G. Feint, "Untersuchungen uber die Abhangigkeit des Umschlages Laminar-turbulent von der Oberflachenrauhigkeit und der Druck verteilung". Jb. 1956 der Schiffbautechn. Gesellschaft 50, 180-203 (1951)
17. See, for example, figure 1 in Ref.9
18. R. Michel, "Etude de la transition sur les profiles d'aile ; establissement d'un critere de determination de point de transition et calcul de la trainee de profile incompressible". ONERA Rep.1/1578A (1951).
19. K. Stewartson, "Correlated compressible and incompressible boundary layers". Proc. Roy. Soc. A 200, pp.84-100 (1949)
20. O. Nonaka, Y. Ishida, M. Sato and H. Kanda, "An Investigation of a Two-Dimensional Hybrid Laminar Flow Control Airfoil at High Subsonic Flow, Part1 : Aerodynamic Characteristic of a Basic Airfoil NLAM78" (In Japanese) National Aerospace Laboratory TR-1076 (1990)
21. A.D. Young and J.H. Paterson, "Aircraft Excresence Drag". AGARD-AG-264 (1981).

This document is provided by JAXA.

APPENDIX

Compressible version of Michel's criterion for transition point

Stewartson's transformation for adiabatic laminar layer converts Michel's criterion in transformed incompressible plane, which is expressed as[18]

$$R_{\bar{\theta}} = f(R_{\bar{x}}) \tag{A1}$$

where $R_{\bar{\theta}} = U_e\bar{\theta}/\nu_\infty$, $R_{\bar{x}} = U_e\bar{x}/\nu_\infty$ and the bar means transformed vatiable, to that for the physical compressible flow plane

$$\frac{\mu_e}{\mu_\infty} R_\theta = f\left[\frac{\mu_e}{\mu_\infty}\left(\frac{T_\infty}{T_e}\right)^3 \frac{\bar{x}}{x} R_x\right] \tag{A2}$$

where $R_\theta = U_e\theta/\nu_e$, $R_x = U_e x/\nu_e$ and $\bar{x}$ is

$$\bar{x} = \int_0^x (T_e/T_\infty)^4 dx.$$

We have expressed the function f(R) as

$$\left.\begin{aligned} f(R) &= 1.535\ R^{0.444} \cdot \exp\ [0.014(\log_{10}R - 5.5) \\ &\quad \times (7.1 - \log_{10}R)],\ (\text{for } 10^{5.5} \leqq R \leqq 10^{7.535}) \\ &= 1.174(1 + 22400/R)\ R^{0.46}, \\ &\qquad (\text{for } R > 10^{7.535},\ R < 10^{5.5}) \end{aligned}\right\} \tag{A3}$$

Equation (A2) with (A3) is the compressible version of Michel's criterion used in the present paper.

This document is provided by JAXA.

TECHNICAL REPORT OF NATIONAL
AEROSPACE LABORATORY
TR-1244T

航空宇宙技術研究所報告1244T号(欧文)

平成6年7月発行

発行所 航空宇宙技術研究所
東京都調布市深大寺東町7－44－1
電話 三鷹(0422)47-5911(大代表) 〒182
印刷所 株式会社 実業公報社
東京都千代田区九段北1－7－8

Published by
NATIONAL AEROSPACE LABORATORY
7-44-1 Jindaijihigashi-machi, Chōfu, Tokyo
JAPAN

This document is provided by JAXA.

Printed in Japan

This document is provided by JAXA.